

CONVECTION MODELS: LABORATORY VERSUS MANTLE *

JOHN A. WHITEHEAD, JR.

Woods Hole Oceanographic Institution, Woods Hole, Mass. (U.S.A.)

(Revised version received March 9, 1976)

ABSTRACT

Whitehead, J.A., 1976. Convection models: laboratory versus mantle. In: O.L. Anderson and B.A. Bolt (editors), *Theory and Experiment Relevant to Geodynamic Processes*. *Tectonophysics*, 35 (1–3): 215–228.

A general comparison is made between some laboratory convection experiments and behavior which the mantle appears to possess. The structure of convection of a uniform viscosity fluid heated evenly from below is reviewed, and is seen to exhibit pronounced three-dimensionality at Rayleigh numbers which are believed to apply to the mantle. Some features which resemble tectonic features are described, but the convection is generally much more complex than the lithospheric plate motions which the earth appears to possess. It is advocated that a new class of problems must be addressed involving surface plate–interior convection interaction. A theoretical stability analysis along these lines is described where each convection cell pushes a rigid plate at the upper surface. Under suitable conditions cells with a large width to depth ratio are predicted to be the most expected form. A second class of experiments and theory is described which is aimed at the problem of a moveable energy source. Under some circumstances the convection in this case goes unstable to a drift which is of the same magnitude as the overturning time of the convection.

INTRODUCTION

In recent years it has become clear that convection is a prime candidate as a mechanism to generate the movement of lithospheric plates. A considerable amount is known about the movement and structure of the plates, while knowledge of movement within the mantle is principally limited to the descending plates under trenches. There are a number of numerical studies being conducted now involving “convection models”, of a two-dimensional vertical slice of fluid. Since most of the descriptive knowledge of our mantle motion involves the structure and motion of the surface plates, it is difficult to find an overlap between these numerical calculations and geophysical observations. In the laboratory it is possible to observe con-

* Contribution number 3646 of the Woods Hole Oceanographic Institution.

vection at high Prandtl and Rayleigh numbers. In the following section some features of laboratory convection will be reviewed. Similarities and differences of the horizontal structure with the mantle convection will be pointed out. In particular, it will be emphasized that the structural features of laboratory convection bear little resemblance to the plate-structure of the mantle problem. It is advocated that it appears necessary to study the interaction between surface features and interior convection. Two such studies, still in their early stages, will be described. In the third section a theoretical study of the stability of convection cells under semi-rigid moveable plates will be reported. Finally, the effects of moveable energy sources on the surface of a fluid will be reviewed.

RAYLEIGH-BÉNARD CONVECTION

This problem has been reviewed in the context of mantle convection by many, including McKenzie, Roberts, and Weiss (1974), Richter (1973a, b), and Richter and Parsons (1975). It has become clear that Bénard convection exhibits a series of discrete transitions to a more complex state as temperature difference is increased. In moderate and large Prandtl number fluid, where Prandtl number is the ratio of dynamic viscosity to thermal diffusivity, two-dimensional rolls adopt a three-dimensional pattern (Krishnamurti, 1970a), which consists of two rolls at right angles (Busse and Whitehead, 1971) and has henceforth been called bimodal flow. A second transition occurs when the convective motions become time-dependent (Krishnamurti, 1970b, 1973). There is good agreement as to the Rayleigh number above which motion is time-dependent between various experiments at low Prandtl numbers but Krishnamurti reports the observation of periodic time-dependent flow above a Rayleigh number of $52,900 \pm 5290$ in fluids with Prandtl numbers of 57, 100, 200, 860, 8600, while Willis and Deardorff (1970) report seeing no oscillations until a Rayleigh number of roughly 100,000 is exceeded in fluids with a Prandtl number of 100. Busse and Whitehead (1974) observed that the oscillations are strongly a function of the structure of the convection planform and that artificially initiated bimodal convection is stationary up to approximately 70,000, 130,000 and 320,000 in fluids with Prandtl numbers of 46, 63, and 126 respectively, while convection which has been allowed to grow from a random background pattern is clearly nonstationary and has a spoke-pattern convection. The only observations of the structure of very high Prandtl number convection are by Richter and Parsons (1975) in which the convection is observed to have a spoke structure. No observations are made of the time-dependent structure. They found that under sufficient shear the convection reverted to rolls aligned with the shear.

In order to clarify the interdependence between structure of the convection and the transition to time-dependent flow, an extensive series of experiments have been recently conducted by Whitehead and Parsons (in preparation) on fluid with a Prandtl number of 8,600, in an apparatus capable

of attaining Rayleigh numbers up to approximately 10^6 . During the course of this study it became clear that the convection can exist in two distinct states — one stationary and one nonstationary,

It was further observed that the time-dependent convection pattern was always spoke-shaped (see Busse and Whitehead, 1974), but spoke-shaped convection was not always time-dependent. We will briefly describe the observed flow here.

The apparatus used is described by Richter and Parsons (1975), and patterned after an apparatus described in Busse and Whitehead (1971). It consisted of a horizontal layer of Dow Corning 200 silicon oil, of viscosity $10 \text{ cm}^2/\text{sec}$, thermometric conductivity — 0.00116, coefficient of expansion — 0.0096, which was bounded above and below by transparent plate glass water manifolds one meter by one meter square. Thermostatically controlled water flowed through each manifold, and thus provided controlled temperature above and below the layer of oil.

A shadowgraph technique was used to visualize convection in the oil layer. It consisted of light from a 5 mm aperture which passed through a series of mirrors, upward through the layer of oil, into another mirror, and onto a frosted screen. The convection bends light of the beam such that cold re-

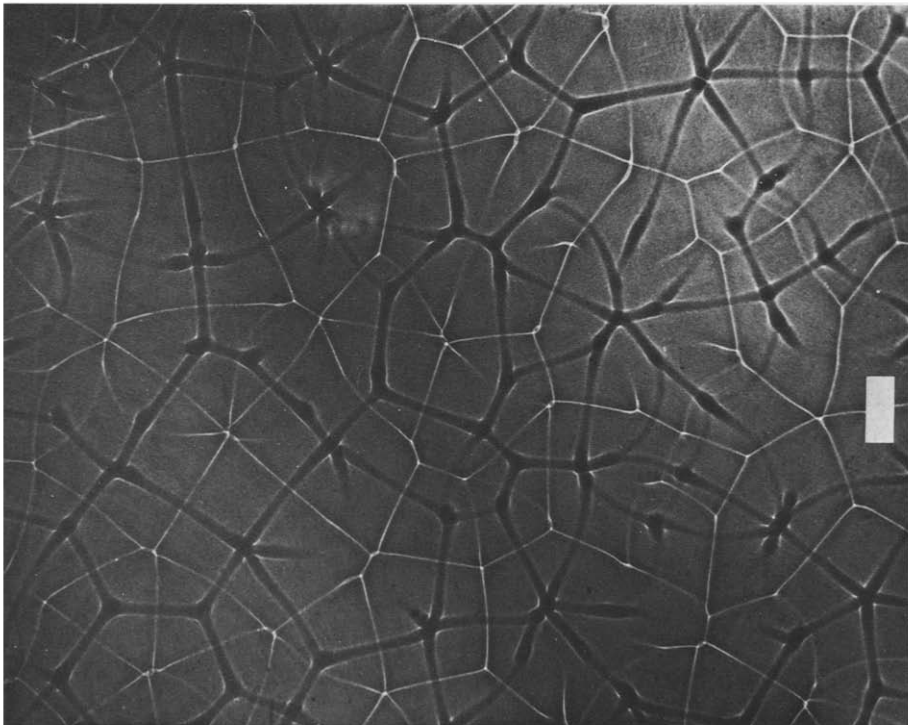


Fig. 1. Photographs of the convection at a Rayleigh number of approximately 500,000. Depth of the fluid layer (7 cm) is marked by the white marker.

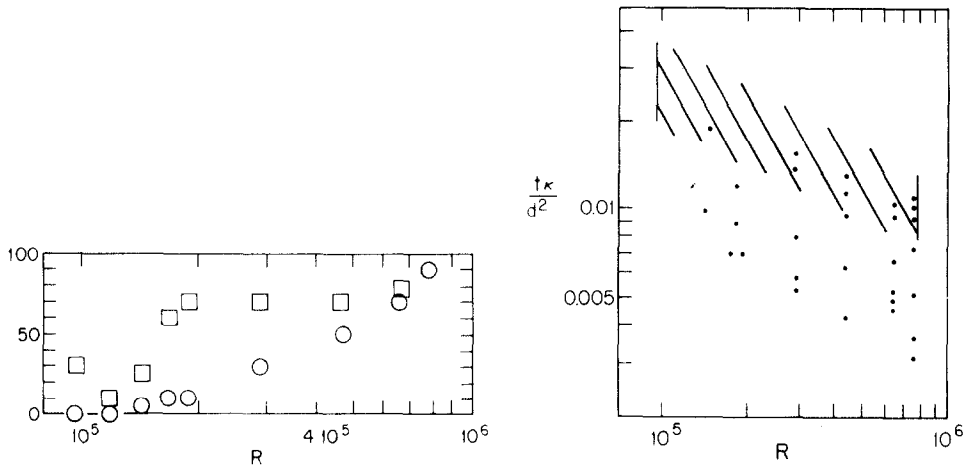


Fig. 2. The estimated percentage of area which contained spoke-shaped convection patterns (squares) and oscillating convection (circles) at various Rayleigh numbers.

Fig. 3. Observations of the turnover time (hatched area), scaled with the time scale d/κ , and oscillation times of the cells. ● = observed oscillations.

gions converge the upward passing light like a convex lens, and hot regions diverge the light like a concave lens. The frosted screen was placed so as to intercept the beam at the distance which gave the most satisfying shadowgraphs, and the shadowgraph was photographed with a 35 mm still and a 16 mm movie camera.

Time lapse movies, filmed at 1/300th normal time, were taken of convection after the apparatus had been held at the desired temperature for at least the previous eight hours. Figure 1 shows a photograph of a typical convective pattern at a Rayleigh number of 780,000, which is within the parameter range of mantle convection. It was found that some regions of the flow had a bimodal structure while other regions had spoke-shaped convection (see Busse and Whitehead (1974) for a description of the collective instability which leads to spoke-shaped convection). In addition, time-dependent oscillations occurred in many spoke-shaped regions. Lastly, the convection pattern was observed to be perpetually changing when spoke patterns existed in any number.

Fig. 2 shows the estimated percentage of area which contained spoke-shaped convection and estimated percentage of the area which had oscillating flow. These estimates were obtained by inspection of time-lapse movies taken over the space of eight hours, and exhibit scatter due to the limited data base.

Fig. 3 shows observations of the turnover time, and oscillation times deduced by observation of the movies with a stop watch. Observations of the turnover time varied by a factor of approximately 4 at the same Rayleigh number and

this was clearly attributable to the variation of velocities in different cell sizes and structures. The time scale is normalized by the factor d^2/κ where d is depth of the fluid and κ is thermal diffusivity. It is clear that the lowest frequency of the oscillations is the turnover frequency, in agreement with observations by Krishnamurti (1970b), but it is not possible to observe the existence of a discrete higher harmonic structure.

Measurements were made of temperature within the fluid by emplacing the temperature probe in the fluid, waiting for five minutes, and then taking a reading. It was clear that the spokes were not merely a local boundary layer structure, but protruded out of the boundary layer to more than half the total depth of the fluid. Experiments using injected dye revealed the same structure. Comparison of the turnover times in Fig. 3 with turnover times in experiments with lower Prandtl number fluids, and with theoretically predicted turnover times revealed good agreement. The values, when extrapolated to Rayleigh numbers which are believed to exist in the mantle of the earth (10^5 – 10^6), can yield times of the order of hundreds of millions of years using reasonable values of the mantle viscosity.

It is difficult to determine whether the oscillations should be expected for Prandtl numbers typical of the mantle (10^{20}) from these data. Comparison of these experiments with experiments at lower Prandtl number reveal a weak Prandtl number dependence for the transition to oscillations, while Krishnamurti reports observing no such dependence. There seem to be three possible causes of the disagreement. One is that the disagreement could be caused by the fact that Krishnamurti's metal boundaries above and below the fluid provide a more uniform temperature boundary condition than our glass. If this is the reason, it means that the oscillations are rather sensitive to boundary conditions (see Fig. 4). Another possible reason is the fact that lateral boundaries tend to be characterized by more oscillations, and Krishnamurti's experiment was in a smaller container. The extra oscillations appear to occur because more spoke-shaped flow exists near boundaries, which can trigger dislocations in bimodal flow. The third possible reason is that the temporal extent of one or both observations are just not adequate, and that

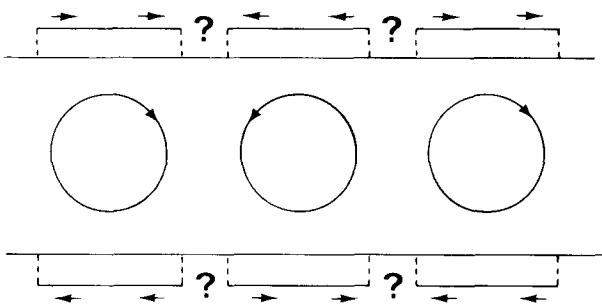


Fig. 4. Sketch of the idealized "floating slab" boundary condition.

we missed a rare, but possible oscillating event at the Rayleigh numbers of 50,000 or so that Krishnamurti reports the emergence of oscillating flow.

Irrespective of the transition to oscillations, the structure of spoke-shaped flow is more complicated than the relatively two-dimensional plate movements observed on the surface of the earth. In addition the distance between spokes was at most a factor of two greater than the depth of the fluid, but it never approached the aspect ratio of cells (order ten or so) which is necessary to satisfy the geophysical observations. It would therefore appear that convection in uniform viscosity fluid is an inadequate first-order model for mantle convection. Many candidates for processes which must be included in this first approximation exist, such as the variation of viscosity, non-Newtonian fluids, phase changes, chemical fractionation. Many of these processes have been parameterized in computer calculations, but the calculations are of a two-dimensional flow and tell nothing about the horizontal planform of the flow. There are cases, however, where greater aspect ratios are found to exist.

In the rest of this paper I will describe two attempts to dynamically couple interior convection to some *surface* process, as a fundamental stability problem that might lead to an understanding of the existing planform. The motivation is simply that we have and are likely to continue to have more observational information about surface features than about convection with depth, and that basic linearized processes must be understood before we can make predictions about horizontal structural planforms.

THE EFFECT OF A RIGID PLATE BEING ADVECTED BY THE FLUID

Richter (1973a, b) has theoretically studied and Richter and Parsons (1975) have experimentally studied the consequences of shear generated by a moving rigid lid upon high Prandtl number convection in a layer of fluid heated from below. It was found that the shear would stabilize roll convection at right angles to the direction of shear, so that the underlying convection would line up along the direction of shear. The author and John Skilbeck (see Appendix) have recently worked upon the problem of the stability of convection in which infinitesimal perturbation convection cells are subjected to boundaries which impose a basic wavelength plus higher harmonics. Motivation was to determine the effects of plates upon underlying convection, plates being manifested by a flow of the form:

$$u = \sum_{n=1}^{\infty} U_n \sin(2n - 1) \alpha x.$$

In practice, the stability of finite sums were found, and the net stress exerted upon the fluid by this flow:

$$\int_0^{\pi} \mu \frac{\partial u}{\partial z} dx$$

was set to zero. The results of the neutral stability calculations are shown in Fig. 5, which also shows the lateral flows which were imposed.

A condition which is most like a "rigid plate" is shown in Fig. 5A, it consisted of the series:

$$U_T(x) = \sum_{n=1}^M U_n \sin(2n-1)\alpha x.$$

where $U_n = (2n-1)^{-1}$. The neutral stability curves for $M = 2, 3$ and 4 are

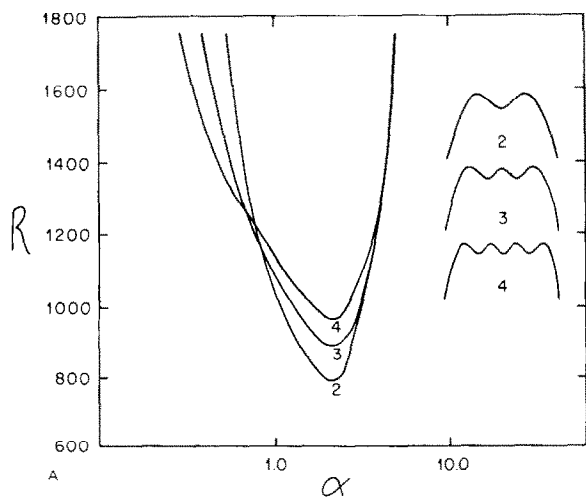


Fig. 5. Neutral stability curve for convection perturbations subjected to the boundary conditions. A. $U_n = (2n-1)^{-1}$.

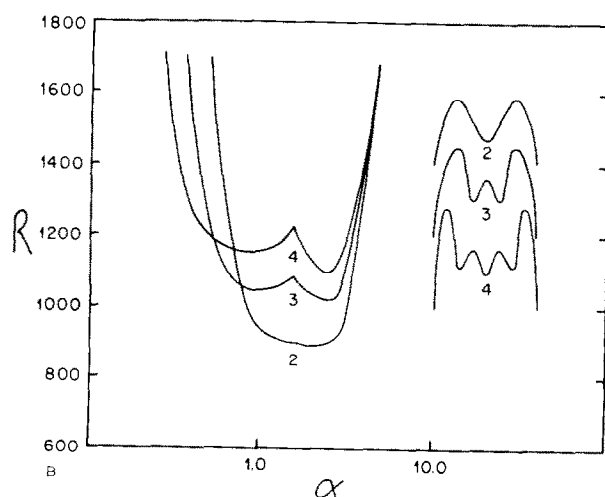


Fig. 5B. $U_n = (2n-1)^{-1/2}$.

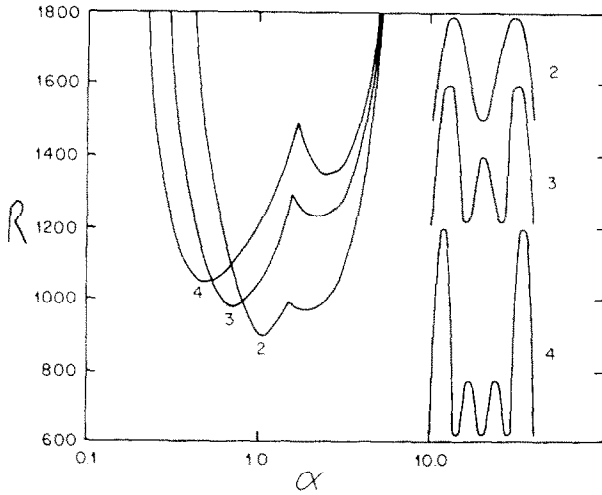


Fig. 5C. $U_n = 1$.

The above cases are shown for $M = 2, 3, 4$.

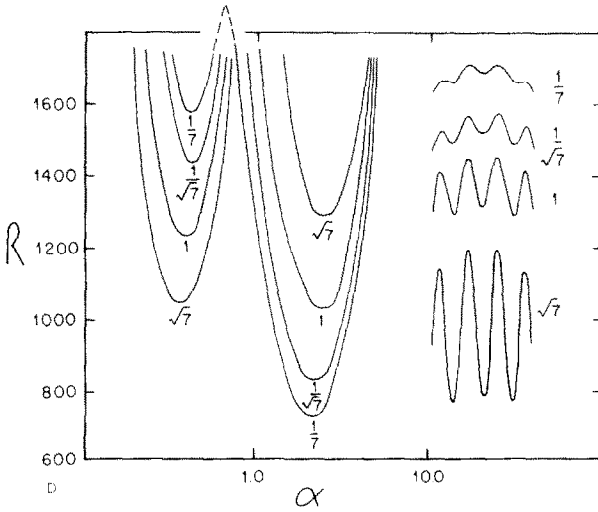


Fig. 5D. $U_1 = 1$, all other $U_n = 0$ except for U_4 which equals $7^{-1}, 7^{-1/2}, 1, 7^{1/2}$, respectively.

wider than the neutral stability curves for “free slip” boundaries, but the wavenumber of the minimum neutral Rayleigh number remained centered at approximately 2. Figures 5B and C show curves when $U_n = (2n - 1)^{-1/2}$, and 1, respectively, for $M = 2, 3$ and 4, and it is evident that the critical wave-

number is lower for greater n in the latter cases. Lastly, Fig. 5D shows a function $U_T(x) = U_1 \sin x + U_4 \sin 7x$, where $U_4 = 7^{-1}$, $7^{-1/2}$, 1, and $7^{1/2}$, respectively.

The calculations indicate that to get wide cells (small wavenumber) we must depart from a rigid plate [$U_n = 1/(2n - 1)$] condition.

SURFACE MODULATION OF HEAT FLUX

A second class of surface—interior feedback processes occurs when convection patterns significantly modify surfaces insulation or heat-source materials. It appears that Elder (1967) was the first to suggest that the continents, in acting as an insulating shield, could generate a new class of lateral motions. A extreme idealization of such a process was analyzed theoretically and studied in the laboratory by Howard et al. (1970), and later by Whitehead (1972). In these studies the insulation—heat source mechanism was replaced by heat sources alone, the heat sources being free to move laterally, and in some cases, up and down.

It was found theoretically and experimentally that such replaced heat sources in a fluid could generate convective motions which in some circumstances could move the sources laterally. One heat source that readily adopted a lateral motion is shown in Fig. 6. It consisted of a styrofoam float 20 cm long with a 2 cm \times 3 cm deep triangular cross-section with a fine heating wire stretched approximately 1 cm below the float. The float in the figure was traveling to the right at a speed of approximately 1 cm/minute. The lateral motion of this float occurs because a thermal tail streams behind the moving float, so that the center of gravity of the density anomaly due to

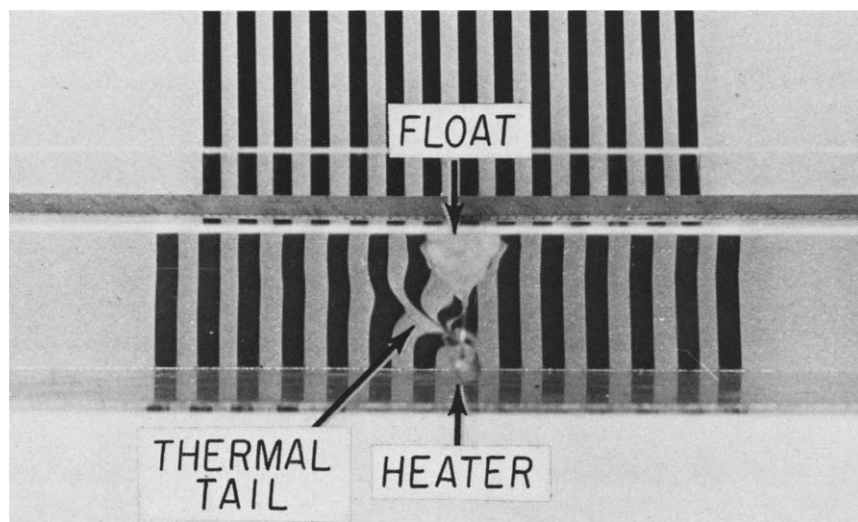


Fig. 6. Photograph of a floating heat source which goes unstable to lateral drifts.

heating lies behind the float. Upwelling which is centered about this center of gravity then pushes the float along.

It was not necessary to have discrete heaters floating in a fluid to predict such effects. An analysis in Whitehead (1972, part 2) predicted that a uniform layer of heat-producing material, when entrapped in downwelling thermals, will generate an oscillating motion. Unfortunately the problem could only be solved approximately because of non-constant coefficients in the equations. The mechanism is schematically shown in Fig. 7. Suppose there is a layer of heat-producing fluid above a deep fluid without internal heat generation. Ultimately the interior fluid would approach an isothermal interior state, with a cooler conductive region above, as shown in the top left. The top boundary layer would then go unstable and plunge downward. The cold heat-producing fluid would then begin to warm up, as there is no boundary close to it to conduct heat away as shown in the lower left. Ultimately it would get warmer than the interior and begin to move upward again, as shown in the lower right.

Koenigsberg (1974, 1975) has recently studied the stability and finite-amplitude properties of a number of different continuously distributed heaters. It was found (1974) that convection with a strong heat source concentration near the bottom would generally tend to uplift the heat sources toward the surfaces while convection with a strong heat source near the top would generally tend to move the heat source downward. In the 1975 study, oscillatory solutions similar to the ones described above were predicted when heat-producing materials on the top surface were free to move only laterally, and it was possible to do the most complete theoretical analysis to data of convection in fluid with a continuously distributed heat source. It was shown that oscillating convection can exist at a lower Rayleigh number than steady convection, and that in one limit a finite-amplitude travelling wave has more heat flux than a standing wave. The travelling wave as analyzed by Koenigsberg is sketched schematically in Fig. 8. The concentration of heat source is sketched in the

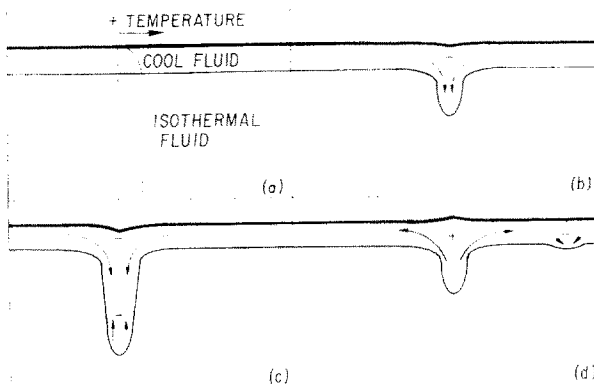


Fig. 7. Idealized scheme of a standing oscillation which is predicted to result from vertical entrapment of heat sources.

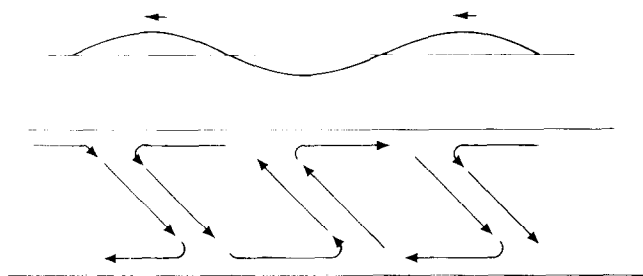


Fig. 8. Sketch of the traveling wave solution found by Koenigsberg. The heat-source distribution is sketched in the top. The heat source is concentrated by surface convergence over the region where fluid is plunging downward. The streamlines are sketched below and exhibit a tilt due to a phase lag generated by the finite time it takes for the thermal signal from the heat sources to travel downward. The pattern is traveling to the left.

top, a few streamlines are sketched on the bottom. The bold arrows denote direction of travel of the convection pattern. It was found that the heat source becomes concentrated in regions where horizontal velocity in the direction of propagation is largest, and that the cold downwelling thermal plunges under the moving source at an angle reminiscent of the trenches plunging under South America and Asia.

CONCLUDING REMARKS

Although this paper opened with a description of the three-dimensional structure of Rayleigh-Bénard convections, the two studies of surface-interior feedback mechanisms have not yet been refined to the point of attacking the question of three-dimensional finite-amplitude convection. The above analyses serve as a fundamental building-block towards the above goal, and quite possibly only when the area of surface-interior interaction has been thoroughly studied will the true processes governing the structure of our present plates, and their interaction with interior convective processes be recognized.

ACKNOWLEDGEMENTS

This research was supported by the Oceanography section, National Science Foundation, NSF grant DES72-01562-A02. John Skilbeck, co-author of the Appendix, received support from the Woods Hole Geophysical Fluid Dynamics Summer Program, supported by the Atmospheric Sciences Section, National Science Foundation, NSF grant DES73-06506.

REFERENCES

- Busse, F.H. and Whitehead, J.A., 1971. Instabilities of convection rolls in high Prandtl number fluid. *J. Fluid Mech.*, 47: 305–320.
- Busse, F.H. and Whitehead, J.A., 1974. Oscillatory and collective instabilities in large Prandtl number convection. *J. Fluid Mech.*, 66: 67–79.
- Chandrasekhar, S., 1961. *Hydrodynamic and Hydromagnetic Stability*. Oxford University Press.
- Elder, J.W., 1967. Convective self propulsion of continents. *Nature*, 214: 657–660.
- Howard, L.N., Malkus, W.V.R. and Whitehead, J.A., 1970. Self-convection of floating heat sources: A model for continental drift. *Geophys. Fluid Dyn.*, 1: 123–142.
- Koenigsberg, M., 1974. *Heat Source Convection*. Geophysical Fluid Dynamics Summer Institute, Fellowship lectures, Woods Hole Oceanographic Institution.
- Koenigsberg, M., 1975. *Convection Waves*. Geophysical Fluid Dynamics Summer Institute, Fellowship lectures, Woods Hole Oceanographic Institution.
- Krishnamurti, R., 1970a. On the transition to turbulent convection, 1. The transition from two to three-dimensional flow. *J. Fluid Mech.*, 42: 295–307.
- Krishnamurti, R., 1970b. On the transition to turbulent convection, 2. The transition to time-dependent flow. *J. Fluid Mech.*, 42 (2): 309–320.
- Krishnamurti, R., 1973. Some further studies on the transition to turbulent convection. *J. Fluid Mech.*, 60 (2): 285–303.
- McKenzie, D.P., Roberts, J.M. and Weiss, N.O., 1974. Convection in the earth's mantle: towards a numerical solution. *J. Fluid Mech.*, 62: 465–538.
- Richter, F.M., 1973a. Convection and the large-scale circulation of the mantle, *J. Geophys. Res.*, 78 (35): 8735–8745.
- Richter, F.M., 1973b. Dynamical models for sea-floor spreading. *Rev. Geophys. Space Phys.*, 11 (2): 223–287.
- Richter, F.M. and Parsons, B., 1975. On the interaction of two scales of convection in the mantle. *J. Geophys. Res.*, 80: 2529–2541.
- Whitehead, J.A., 1972. Moving heaters as a model of continental drift. *Phys. Earth Planet. Inter.*, 199–212.
- Willis, G.E. and Deardorff, J.W., 1970. The oscillatory motions of Rayleigh convection. *J. Fluid Mech.*, 44: 661–672.

APPENDIX

Stability of a motionless fluid under periodic, rigid plates which are free to move laterally by J.A. Whitehead, Jr., Department of Physical Oceanography, Woods Hole Oceanographic Institution, and John Skilbeck, Department of Geodesy and Geophysics, University of Cambridge

The stationary perturbation to a motionless infinite horizontal layer of fluid heated from below obeys the well-known dimensionless equations (see Chandrasekhar, 1961, Chapter II):

$$(D^2 - a^2)^3 w = -Ra^2 w \quad (1)$$

where $D \equiv \partial/\partial z$, z is the direction of gravity, a is the horizontal wavenumber, and w is vertical velocity of the fluid. We will assume that the perturbation is subjected to the zero vertical velocity and zero temperature boundary conditions:

$$w = (D^2 - a^2)^2 w = 0 \quad (2a)$$

and that a horizontal sinusoidal velocity is imposed above and below each cell:

$$Dw = \pm aU \sin ax \text{ at } z = \pm 1/2 \tag{2b}$$

where U is a constant. We imagine for the moment that we impose this forced flow by some suitable mechanism. A general solution of eq. 1 is:

$$w = A \cos q_0 z + B \cosh qz + C \cosh q^* z \tag{3}$$

where:

$$q_0 = a(\tau - 1)^{1/2}$$

$$\text{Re}(q) = a\left[\frac{1}{2}(1 + \tau + \tau^2)^{1/2} + 1/2(1 + \frac{1}{2}\tau)\right]^{1/2}$$

$$\text{Im}(q) = a\left[\frac{1}{2}(1 + \tau + \tau^2)^{1/2} - \frac{1}{2}(1 + \frac{1}{2}\tau)\right]^{1/2}$$

$$\tau = (R/a^4)^{1/3}$$

and the constants A, B, C are solutions to the matrix equation generated by substituting solution (3) into the boundary conditions (2), i.e.:

$$\begin{vmatrix} \cos \frac{q_0}{2} & \cosh \frac{q}{2} & \cosh \frac{q^*}{2} \\ (q_0^2 - a^2)^2 \cos \frac{q_0}{2} & (q^2 - a^2) \cosh \frac{q}{2} & (q^{*2} - a^2)^2 \cosh \frac{q^*}{2} \\ -\frac{q_0}{a} \sin \frac{q_0}{2} & \frac{q}{a} \sinh \frac{q}{2} & \frac{q^*}{a} \sinh \frac{q^*}{2} \end{vmatrix} \begin{vmatrix} A \\ B \\ C \end{vmatrix} = \begin{vmatrix} 0 \\ 0 \\ U \end{vmatrix}$$

The force that our imaginary external mechanism must exert to keep a stationary state is:

$$\tau = \mu \frac{\partial u}{\partial z} = \frac{\mu}{a} D^2 w$$

where μ is viscosity.

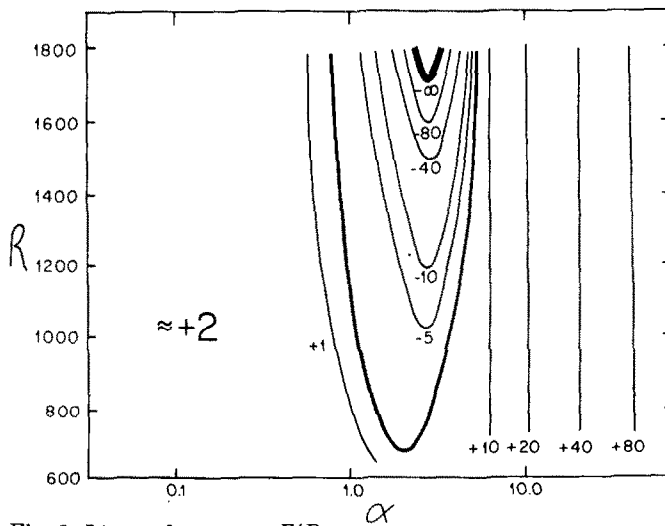


Fig. 9. Lines of constant F/R_d .

After solving for $A, B,$ and C above, and using these values in (3), and taking the second derivative, the above equation reduces to:

$$\tau = \mu \frac{F}{R_d} U \sin ax$$

where F is the function of R and a which is ordinarily set to zero to solve for the stability of a fluid with zero stress (so-called “free”) boundary conditions, and R_d is the function of R and a which is ordinarily set to zero to solve for the stability of a fluid with a zero lateral velocity (so-called “rigid”) boundary condition (equation 216 in Chandrasekhar). The parameter group F/R_d can be determined analytically to be:

$$\frac{F}{R_d} = \frac{37a^2}{q_0 \tan \frac{q_0}{2} + \frac{1 - i\sqrt{3}}{2} q \tanh \frac{q}{L} + \frac{1 + i\sqrt{3}}{2} q^* \tanh \frac{q^*}{2}} \tag{4}$$

and is plotted in Fig. 9. Three regions are evident. Below the bottom bold curve, F/R_d is negative, which means that if a velocity is imposed, the fluid exerts a resistance to that flow. One must put energy into the mechanism to keep a stationary flow pattern. Between the bottom and top bold curves, F/R_d is positive, due to the function F changing sign across the bottom bold curve. This means that if a velocity is imposed the convecting fluid pulls that displacement. One must brake the mechanism to keep a stationary flow pattern, and take energy out of the flow pattern.

Let us suppose now that there exists some mechanism which drives a number of wavelengths, all multiples of some basic wavelength. We will specify the mechanism as a finite sum of modes:

$$U_T = \sum_{n=1}^M U_n \sin(2n - 1)\alpha x \tag{5}$$

Since the equation set (1) and (2) are linear, the stress diagram Fig. 9 remains valid for each mode upon the substitution of U_n for U , and $(2n + 1)\alpha$ for α . We can now solve for the positive or negative stress that each mode exerts upon the mechanism between the interval of the longest wavelength, and it is:

$$\int_0^{\pi/\alpha} \tau dx = \int_0^{\pi/\alpha} \mu \left. \frac{\partial u}{\partial z} \right|_{z=1/2} dx = \frac{\mu}{(2n - 1)\alpha^2} \frac{F[(2n - 1)\alpha, R]}{R_d[(2n - 1)\alpha, R]} U_n$$

It is possible for us to use Fig. 9 to determine this stress. Lastly, in order to make this a stability problem, we assume that all the forces upon the mechanism add up to zero. This defines a curve in R, α space for each different mechanism, which can be interpreted as a neutral stability curve of perturbations subjected to the stated kinematic boundary condition. We have solved this problem for a number of different boundary mechanisms, and some of the results will be given here. The first mechanism was defined by $U_n = 1/(2n - 1)$. This function approaches a train of step functions as M goes to infinity. Figure 5A shows the neutral stability curve for $M = 2, 3,$ and 4 . The most prominent feature is that the width of neutral solutions gets wider as M is increased. Figures 5B and C show the neutral stability curves for $U_n = (2n - 1)^{-1/2}$, and 1 , respectively, with $M = 2, 3,$ and 4 . These mechanisms have more energy in the higher harmonics, and the surface velocities U_T are sketched in the figures. The bandwidth of the solutions is wider, and a low wavenumber minimum (implying a long wavelength) develops. Figure 5D shows the neutral stability curve for a boundary condition $U_T(a) = U_1 \sin x + U_4(a) \sin 7x$, where U_4 was made to be $7^{-1}, 7^{-1/2}, 1,$ and $7^{1/2}$, respectively. Again long wavelengths were seen when U_4 was large.

If finite-amplitude convection with rigid upper slabs prefer this mode of flow, it is a possible explanation for the large size of plates on the earth relative to the depth of the mantle.